Science of the Total Environment 599–600 (2017) 2074–2084

Contents lists available at ScienceDirect

Science of the Total Environment

journal homepage: www.elsevier.com/locate/scitotenv

Spatiotemporal characteristics of $PM_{2.5}$ and PM_{10} at urban and corresponding background sites in 23 cities in China

Lizhong Xu [a], Stuart Batterman [b,*], Fang Chen [c], Jiabing Li [a], Xuefen Zhong [d], Yongjie Feng [e], Qinghua Rao [c], Feng Chen [f]

[a] College of Environmental Science and Engineering, Fujian Normal University, Fuzhou 350007, China
[b] School of Public Health, University of Michigan, Ann Arbor, MI 48104, United States
[c] College of Ocean Science and Biochemistry Engineering, Fuqing Branch of Fujian Normal University, Fuqing 350300, China
[d] Fujian Provincial Academy of Environmental Sciences, Fuzhou 350007, China
[e] Henan Langtian Environmental Protection Technology Company, Zhengzhou 450000, China
[f] Fuzhou Environmental Monitoring Station, Fuzhou 350007, China

HIGHLIGHTS

- Severe air pollution episodes are frequent in many Chinese cities.
- $PM_{2.5}$ and PM_{10} levels in 23 cities at 178 urban and 23 urban contrast sites are studied.
- PM concentrations frequently exceed Chinese standards, especially in winter.
- Levels in cities are only moderately higher than levels at corresponding contrast sites.
- Exurban and regional sources of $PM_{2.5}$ require control to meet air quality goals.

GRAPHICAL ABSTRACT

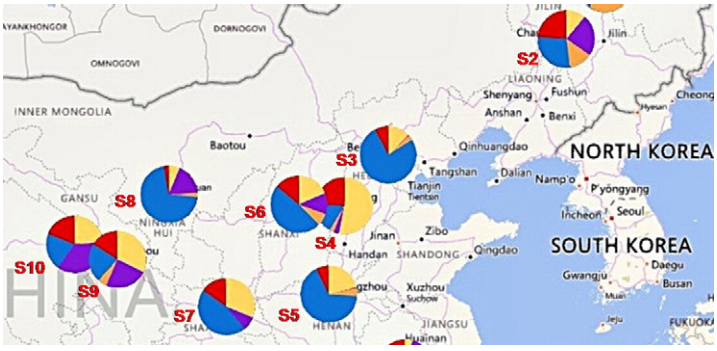

ARTICLE INFO

Article history:
Received 7 February 2017
Received in revised form 5 May 2017
Accepted 5 May 2017
Available online 25 May 2017

Editor: D. Barcelo

Keywords:
Air quality, particulate matter
Spatial variation
Temporal variation
Urban background
China

ABSTRACT

Air pollution episodes in China are frequent and a more comprehensive understanding of pollution sources and impacts is needed to design appropriate strategies and set emission reduction targets. This study analyzes $PM_{2.5}$ and PM_{10} concentrations measured in 23 cities at 178 urban sites and at 23 corresponding "urban contrast" sites in China with the goals of understanding spatial and temporal trends and quantifying the regional component of PM pollution. The contrast sites, located an average of 29 km from cities in the upwind direction, are intended to represent "background" levels. Using daily measurements from April 2013 to March 2014, we assess compliance with air quality standards, $PM_{2.5}/PM_{10}$ ratios and urban "increments," defined as the increase in PM levels in the city compared to the contrast site. Spatial and temporal patterns at daily, monthly and annual levels are shown using distributions, correlations, spatial autocorrelation, and factor analyses. At the contrast sites, $PM_{2.5}$ and PM_{10} concentrations averaged 56 ± 26 and 91 ± 44 μg m^{-3}, respectively, and China's daily and annual average air quality standards were frequently exceeded. $PM_{2.5}$ and PM_{10} concentrations in most cities exceeded levels at the corresponding contrast sites, but by an average of only 14 ± 14 and 26 ± 27 μg m^{-3}, respectively. Seasonal changes in $PM_{2.5}$ and PM_{10} concentrations and urban increments were striking, e.g., levels increased 2 to 3-fold in winter at several sites. The significance of exurban and regional sources of $PM_{2.5}$ is demonstrated by the small

* Corresponding author at: University of Michigan, School of Public Health, 1420 Washington Heights, Ann Arbor, MI 48104, United States.
E-mail address: stuartb@umich.edu (S. Batterman).

http://dx.doi.org/10.1016/j.scitotenv.2017.05.048

urban increments, the strong correlations across broad regions, and the correlation between daily levels at city and contrast sites. These sources will require control to achieve air quality goals, in particular, the PM_{10} and $PM_{2.5}$ targets announced by the Chinese government in 2013.

1. Introduction

Exposure to air pollution is considered to be the world's largest environment health risk (Jakubiak-Lasocka et al., 2015; Xia et al., 2015; Wallner et al., 2014; Yorifuji et al., 2016; Yang et al., 2016a; Yang et al., 2016b), causing an estimated 7 million deaths each year, equivalent to one in eight deaths across the globe (WHO, 2016). Particulate matter (PM), including $PM_{2.5}$ (particles with aerodynamic diameter ≤2.5 μm) and PM_{10} (≤10 μm), is a major concern in many countries including China, the focus of the present paper. $PM_{2.5}$ concentrations in China often far exceed the national ambient air quality standard (GB3095-2012 Grade II) (Zhou et al., 2016), which is equivalent to the WHO Interim Target One (IT-1). Residents of northern China have an estimated mean life expectancy 5.5 years lower than those in southern China, a result of elevated rates of cardiorespiratory mortality due to PM exposure (Chen et al., 2013). In the central Beijing area alone, mortality attributed to $PM_{2.5}$ causes an estimated 5100 deaths per year for the 2001–2012 period, and the all-age mortality rate due to $PM_{2.5}$ exposure was 15 per 10,000 person-years for the 2010–2012 period (Zheng et al., 2015).

Actions taken by the Chinese government to address air pollution include increasing the stringency of ambient standards (e.g., GB 3095-2012), strengthening emission control measures, and implementing a national ambient air quality monitoring network. Since January 2013, this network has measured hourly concentrations of six pollutants at multiple sites in over 338 cities. Monitoring sites are classified as "urban assessment" sites, which are distributed in built-up areas of cities, or as "urban contrast" sites, which are located in the predominantly upwind direction and usually >10 km from the city's population core and pollution sources (Ministry of Environmental Protection of the People's Republic of China, 2012). Air pollutant levels at contrast sites are intended to represent "background" levels, i.e., concentrations that would result with minimal or fully controlled emissions in the city. The public can access real-time air quality data, and many non-governmental "unofficial" websites (BestApp Studio, 2016; Wang, n.d.) use these data to show daily and monthly trends.

Since 2014, Chinese has had two sets of air quality standards. The Grade I standards apply to special regions (e.g., natural reserves, scenic resorts), and specify $PM_{2.5}$ and PM_{10} 24-hour mean concentrations of 35 and 50 μg m^{-3}, respectively, and annual means of 15 and 40 μg m^{-3}. These standards are similar to the WHO Interim Target Three (IT-3) guidelines. The Grade II standards apply to general areas, and are equivalent to WHO Interim Target One (IT-1) with $PM_{2.5}$ and PM_{10} 24-hour means of 75 and 150 μg m^{-3}, respectively, and annual means of 35 and 70 μg m^{-3} respectively (WHO, 2005). The draft Chinese Air Quality Index uses six classifications based on 24-h average concentrations: "excellent" ($PM_{2.5}$ ≤ 35 μg m^{-3}; PM_{10} ≤ 50 μg m^{-3}), "favorable" (35 < $PM_{2.5}$ ≤ 75 μg m^{-3}; 50 < PM_{10} ≤ 150 μg m^{-3}), "lightly polluted" (75 < $PM_{2.5}$ ≤ 115 μg m^{-3}; 150 < PM_{10} ≤ 250 μg m^{-3}), "moderately polluted" (115 < $PM_{2.5}$ ≤ 150 μg m^{-3}; 250 < PM_{10} ≤ 350 μg m^{-3}), "heavily polluted" (150 < $PM_{2.5}$ ≤ 250 μg m^{-3}; 350 < PM_{10} ≤ 420 μg m^{-3}), and "ultra-seriously polluted" ($PM_{2.5}$ > 250 μg m^{-3}; PM_{10} > 420 μg m^{-3}).

Air pollution research in China pertaining to ambient PM has expanded, and includes analyses of spatiotemporal variation (Peng et al., 2016; Seltenrich, 2016), source apportionment (Zíková et al., 2016; Zhang et al., 2015; Wang et al., 2015; Tan et al., 2014; Zheng et al., 2005), chemical characterization (Zhang et al., 2016a; Yang et al., 2016c) and health effects (Zhou et al., 2013; Sun et al., 2013). Most attention has focused on the larger cities, e.g., Beijing (Wen et al., 2016; Yang et al., 2016d), Shanghai (Wang et al., 2016a; Wang et al., 2013; Fu et al., 2010), Guangzhou (Wang et al., 2016b; Jahn et al., 2013; Tan et al., 2009), Shenzhen (Zhang et al., 2016b) and Xi'an (Xu et al., 2016; Shen et al., 2016). A few studies have used satellite-derived aerosol optical depth (AOD) (Ma et al., 2016; Zheng et al., 2016; Yang et al., 2016e; Yong-Ze et al., 2015), which is correlated to (and calibrated using) ground-level monitoring data. While some research has focused on air quality in rural or "background" areas where $PM_{2.5}$ levels also are elevated (Yao et al., 2016; Lai et al., 2016; Zhao et al., 2009), a systematic understanding of pollutant levels in both urban and exurban/rural areas is needed to quantify the role of urban and regional emission sources, to formulate realistic goals for pollution control and, more generally, to inform air quality management.

This study examines the spatial and temporal variation and relationship between $PM_{2.5}$ and PM_{10} concentrations at urban and contrast sites in 23 Chinese cities. Our primary objective is to analyse the influence of background concentrations of $PM_{2.5}$ and PM_{10} on Chinese cities. As noted, prior work on this topic has been limited.

2. Methods

2.1. Monitoring sites

The Chinese national monitoring network includes over 338 cities, but not all cities have a contrast site. Initially, 37 cities with contrast sites with largely complete data for the period of interest (1 April 2013 to 31 March 2014) were selected. Of these, seven of the city-contrast site pairs had fewer than 70% of days (260 days) reporting valid daily observations of either $PM_{2.5}$ or PM_{10} during the study period; these were excluded. After mapping the sites, seven contrast sites were found to be within 10 km of cities and thus potentially influenced by urban emissions; these sites also were excluded. The remaining 23 city-contrast pairs, shown in Fig. 1 and in supplementary materials (SM Fig. S1), are located in 21 provinces. Each city had an average of 8 monitoring sites (total of 178 urban sites in the selected cities, excluding its contrast site).

2.2. Data analysis

Monitoring sites were classified using several approaches. Initially, cities were divided into northern (10 cities) and southern (13 cities) regions by the demarcation line of the Qingling Mountain and its eastern extension to the Huaihe River. Second, using a new economic classification of provinces, cities were grouped into eight regions: northeast, northern coastland, Yellow River middle reaches, northwest, southwest, southern coastland, eastern coastland, and Yangtze River middle reaches (National Bureau of Statistics of China, 2016). These regions were further aggregated to four larger regions: east, middle, west and northeast, which respectively contain 8, 6, 7 and 2 of the study cities. Table 1 lists characteristic of the cities and regions. Factor analysis (described below) also was used to identify alternative site groupings.

Polluted periods were defined using the Grade II standards (35 and 75 μg m^{-3} for annual and daily levels of $PM_{2.5}$; 70 and 150 μg m^3 for annual and daily averages of PM_{10}). These standards apply to both urban and contrast sites. Annual average concentrations were calculated at each site if at least 70% (260 observations) of daily measurements were valid. City-wide daily concentrations were calculated if at least

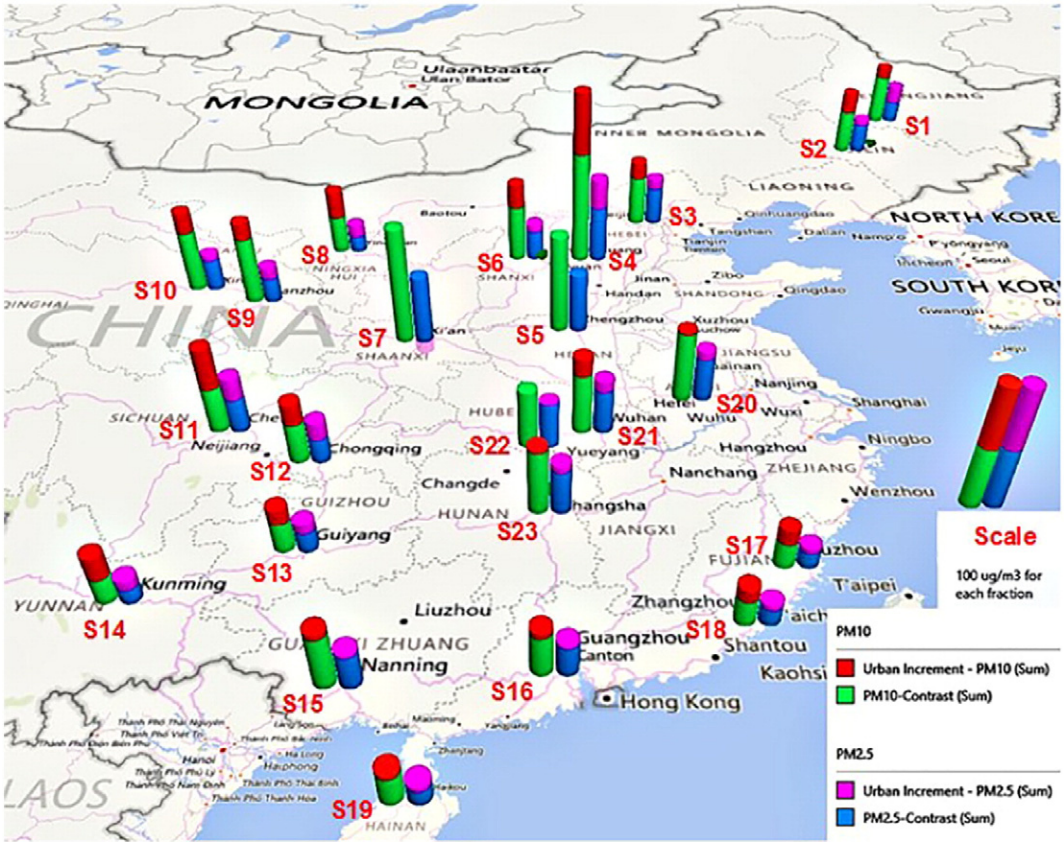

Fig. 1. Annual average PM_{10} and $PM_{2.5}$ concentrations at 23 cities. Total bar height represents concentration; left bar in pair shows PM_{10} concentration at the contrast site and the urban increment; right bar in pair is for $PM_{2.5}$. Site identifiers shown in Table 1.

70% of the city's sites had valid daily averages; city-wide annual averages were determined by averaging these concentrations if at least 70% of the city-wide daily averages were valid. All sites met these criteria. The coefficient of variance (COV) was used to assess the homogeneity of annual average concentrations among urban sites in each city. The "urban increment" was calculated as the difference in daily

Table 1
Details of urban and contrast sites. "Number sites" is number of monitoring sites in the urban area. Distance is approximate distance between contrast site and urban center. Direction refers to the direction of contrast site relative to the urban center.

Site				Region		Number	Contrast sites		
Code	City	Lattitude (°N)	Longitude (°E)	N-S	E-W	Sites	Location	Distance (km)	Direction
S1	Harbin	45.75	126.63	N	NE	11	Lingbei	10	W
S2	Changchun	43.92	125.30	N	NE	9	Suaiwanzi	40	SSE
S3	Beijing	39.90	116.47	N	E	11	Dingling	50	NNW
S4	Shijiazhuang	38.05	114.43	N	E	7	Fenglongshan	20	SW
S5	Zhengzhou	34.73	113.70	N	M	8	Ganglishuiku	20	NNW
S6	Taiyuan	37.85	112.55	N	M	8	Shanglan	20	NNW
S7	Xi'an	34.25	108.92	N	M	12	Chaotan	15	NNW
S8	Yinchuan	38.47	106.22	N	W	5	Helansanmaliankou	30	NW
S9	Lanzhou	36.05	103.83	N	W	4	Yuzhonglanda	40	ESE
S10	Xining	36.62	101.82	N	W	3	Diwushuichang	20	WNW
S11	Chengdu	30.65	104.07	S	W	7	Lingyanshi	60	NW
S12	Chongqing	29.55	106.55	S	W	17	Jinyunshan	30	NNW
S13	Guiyang	26.57	106.72	S	W	9	Tongmuling	40	SSE
S14	Kunming	25.05	102.70	S	W	6	Xishan	15	WSW
S15	Nanning	22.78	108.35	S	W	7	Xianhu	10	E
S16	Guangzhou	23.12	113.26	S	E	11	Maofengshan	60	NNE
S17	Fuzhou	26.08	119.28	S	E	4	Gushan	10	SE
S18	Xiamen	24.43	118.07	S	E	3	Xidong	40	N
S19	Haikou	20.05	110.17	S	E	4	Dongzaigang	30	SE
S20	Hefei	31.85	117.27	S	M	9	Dongpushuiku	15	WNW
S21	Wuhan	30.62	114.33	S	M	9	Chenghuqihao	50	SW
S22	Changsha	28.20	112.92	S	M	9	Shaping	20	N
S23	Zhuzhou	27.83	113.13	S	M	5	Dajing	12	E
–	Average	–	–	–	–	7.7	–	28.6	–

and annual concentrations in the city compared to levels at the corresponding contrast site. Descriptive statistics including histograms were calculated for these increments at each city. The spatial autocorrelation of $PM_{2.5}$, PM_{10} and concentration increments were evaluated using Moran's I and Geary's C indices. Seasonal average statistics were defined for winter (Dec. – Feb.), spring (Mar. – May), summer (June – Aug.) and fall (Sept. – Nov.).

Average concentrations in each region were calculated. Site groups were also identified using factor analyses, daily data, and the (absolute value of) factor loadings that exceeded an absolute value of 0.5. This analysis used both Spearman and Pearson correlation coefficients, Varimax rotations, the number of factors based on Eigenvalues exceeding 1, and a 5-day running average of PM levels (to account for transport between sites). To increase robustness, multiple imputation ($n = 5$) was used to generate a complete data set. Sensitivity analyses examined these procedures. $PM_{2.5}/PM_{10}$ ratios and contrast/city ratios were calculated, and stratified by decile, month and season. Day-of-week and weekend-weekday differences were examined using medians calculated for each site and pollutant. Due to the skewness of the daily data, non-parametric statistical measures were used, e.g., Spearman correlation coefficients and Mann-Whitney tests.

Multiple checks were conducted to ensure data quality. Air quality data for the period, obtained from public websites (PM2.5 Real-time Monitoring Net, Fujian, China, 2013), were checked prior to use by comparing to the national monitoring network. These data were validated by the China National Environmental Monitoring Center (Ministry of Environmental Protection of the People's Republic of China, 2013). Wang et al., (2014) used the same data source to analyse the spatial and temporal variation in 31 provincial cities; our data matched this analysis. Data pairs where the $PM_{2.5}$ level exceeded 120% of the PM_{10} levels (if both exceeded 10 μg m^{-3}) were deleted, and $PM_{2.5}/PM_{10}$ ratios and contrast/urban PM ratios were calculated only if concentrations exceeded 10 μg m^{-3}. These procedures removed only a few observations but eliminated spuriously high ratios. Finally, we confirmed that our data matched official annual environmental statements for each city (SM Table S1).

3. Results

Table 1 lists the monitoring sites and details of the urban and contrast sites. Contrast sites were an average of 28.6 km from city centers. In the northern region, contrast sites were mostly north (N) or west (W) of the corresponding city. In the southern region, directions varied, reflecting prevailing wind directions. The 23 site-pairs spanned the more populated eastern portion of China (SM Fig. S1).

3.1. Annual average PM levels

Annual average concentrations and urban increments at the 23 cities are depicted in Fig. 1. Site S4 (Shijiazhuang) had by far the highest $PM_{2.5}$ and PM_{10} concentrations (148 and 295 μg m^{-3} respectively); its contrast site had the third highest $PM_{2.5}$ (96 μg m^{-3}) and the second highest PM_{10} (166 μg m^{-3}) concentrations. Considering $PM_{2.5}$, levels across the 23 contrast sites averaged 56 ± 26 μg m^{-3} (range: 28 μg m^{-3} at S14 Kunming to 117 μg m^{-3} at S7 Xi'an); levels across the 23 cities averaged 70 ± 27 μg m^{-3} (range: 33 μg m^{-3} at S19 Haikou to 148 μg m^{-3} at S4 Shijiazhuang); and the urban increment averaged 14 ± 14 μg m^{-3} (SM Table S2). Concentrations at contrast sites represented 78 ± 18% of city levels, however, excluding the three sites (S5, S7, S22) where contrast sites may be inappropriately located (see below), this percentage fell to 72 ± 20%. $PM_{2.5}$ concentrations at monitors within a city were quite uniform, e.g., COVs averaged 8.9% across the 23 cities. Concentrations at northern sites exceeded levels in the south by an average of 19 μg m^{-3} at both contrast and city sites. The Grade II $PM_{2.5}$ annual average air quality standard (35 μg m^{-3}) was exceeded in 21 of 23 cities and at 17 of 23 contrast sites. (Contrast sites S8, S13–14, S19, S17–18 met this standard.) In the cities, only 12 of the 178 monitoring sites met the standard (2 in Kunming, 4 in Fuzhou, 2 in Xiamen, and 4 in Haikou).

For PM_{10}, concentrations at contrast and city sites averaged 91 ± 44 and 116 ± 50 μg m^{-3}, respectively, a difference of 26 ± 27 μg m^{-3}. Concentrations at contrast sites represented 78 ± 18% of city levels, or 70 ± 21% after excluding the three sites noted earlier. Again, PM_{10} concentrations in the north exceeded levels in the south (by an average of 48 and 58 μg m^{-3} at contrast and urban sites, respectively), and PM_{10} levels across individual cities were similar (COVs averaged 8.5% across the 23 cities). Only 8 of the 23 contrast sites (S8, S12–14, S16–19) and 16 urban sites (3 in Guiyang; 1 in Kunming; 2 in Guangzhou; 3 in Fuzhou; 3 in Xiamen; 4 in Haikou) attained the Grade II standard (70 μg m^{-3}).

Across the cities, annual average $PM_{2.5}$ and PM_{10} levels were strongly correlated ($r = 0.89$ at urban sites and $r = 0.90$ at contrast sites). $PM_{2.5}$ levels at city and contrast sites were highly correlated ($r = 0.84$), as were PM_{10} levels ($r = 0.84$; SM Fig. S2).

The urban increments averaged 14 ± 14 and 26 ± 27 μg m^{-3} for $PM_{2.5}$ and PM_{10}, respectively, and increments showed a tendency to increase with concentration (Fig. 2A). At 20 site-pairs, city levels were

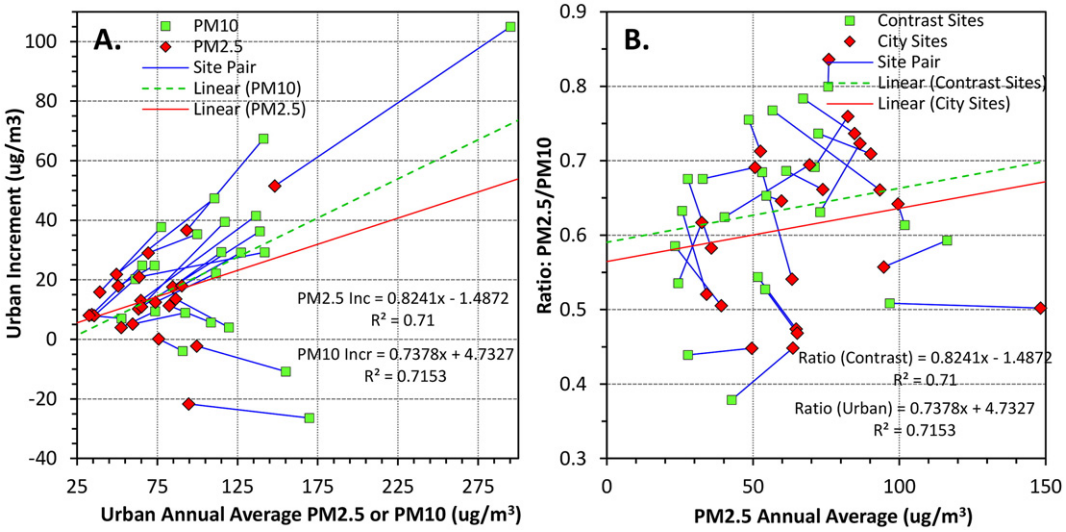

Fig. 2. (A). $PM_{2.5}$ and PM_{10} urban increments at the 23 cities and contrast sites. Site pairs linked by lines. Regression lines and equations shown for $PM_{2.5}$ and PM_{10} increments. (B) Ratio of $PM_{2.5}/PM_{10}$ concentrations at the 23 cities and contrast sites. Site pairs linked by lines. Regression lines and equations shown for ratios.

higher than the corresponding contrast site, as expected. For $PM_{2.5}$, S4 Shijiazhuang and S12 Chongqing had the highest increments (52 and 37 μg m^{-3} higher, respectively); for PM_{10}, S4 (again) and S11 Chengdu had the highest increments (105 and 67 μg m^{-3}, respectively), suggesting substantial emission sources in these cities. In contrast, three site-pairs (S5 Zhengzhou, S7 Xi'an, S22 Changsha) had higher concentrations at the contrast site (shown by negative increments in Fig. 2A), especially S7 Xi'an where $PM_{2.5}$ and PM_{10} levels at the contrast sites were 22 and 26 μg m^{-3} higher, respectively. This unanticipated result probably results from nearby or upwind emissions at the contrast site, e.g., construction, traffic, industry or agricultural burning. Excluding these three site-pairs, $PM_{2.5}$ and PM_{10} urban increments averaged 16 ± 12 and 30 ± 24 μg m^{-3}, respectively, equivalent to 24 and 26% of urban levels, respectively.

$PM_{2.5}/PM_{10}$ ratios at each site pair are shown in Fig. 2B. In cities, $PM_{2.5}$ represented over half of PM_{10} at 19 of the 23 cities with average $PM_{2.5}/PM_{10}$ ratio of 0.61 ± 0.11; and $PM_{2.5}$ was also dominant at 21 of the 23 contrast sites with an average ratio of 0.63 ± 0.11. $PM_{2.5}/PM_{10}$ ratios tend to increase at sites with higher $PM_{2.5}$ concentrations, and ratios at city and contrast sites were correlated and generally similar, e.g., site-pairs S3, S16, and S21–22 had higher ratios (above 0.7) at both city and contrast sites, while S4 and S8–9 had lower ratios (below 0.5). With the exceptions of sites S4 and S8–9, $PM_{2.5}$ constituted the bulk of PM_{10}.

Annual average $PM_{2.5}$ and PM_{10} concentrations in nearby cities had positive spatial autocorrelation, e.g., Moran's I exceeded 0.5 for site pairs within 500 km, while concentrations in distant cities were negatively but weakly correlated, e.g., $I < -0.2$ for site pairs separated by over 1000 km (SM Table S3). The Geary C index, another spatial autocorrelation metric that is more sensitive to differences in small neighborhoods (Lai et al., 2009), showed similar but somewhat muted trends. In contrast, urban increments of both $PM_{2.5}$ and PM_{10} showed negligible spatial autocorrelation, possibly because the increments depended on varying and city-specific factors; alternatively, PM levels at the contrast sites might be influenced by relatively large, varying and unknown emission sources. For $PM_{2.5}$ and PM_{10}, however, the spatial autocorrelation results support site groupings by proximity.

The spatial autocorrelation varied by season and region. Autocorrelation was lowest in winter and highest in summer; this applied to both $PM_{2.5}$ and PM_{10} at both urban and contrast sites. Summer average PM levels at contrast sites had particularly high spatial autocorrelation (e.g., $I = 0.84$ and 0.86 for $PM_{2.5}$ and PM_{10}, respectively (SM Table S3)). In summer, the relative variation (e.g., COV) of PM levels among the 23 cities was the highest; again, this applied to $PM_{2.5}$ and PM_{10} at both urban and contrast sites (SM Table S2). Regional analyses of spatial autocorrelation using separate analyses for the northern and southern regions showed high spatial autocorrelation among nearby sites (within 500 km) in the southern region (I from 0.57 to 0.73), but much lower autocorrelation in the northern region (I from −0.08 to 0.35), suggesting that autocorrelation results were driven, in part, by north-south differences. However, robustness of these results is restricted due to the limited number and coverage of sites in the regional analyses, which give a small number of pairs of neighbors (e.g., only 12 pairs in the 0–500 km bin).

Fig. 1 (and SM Fig. S3) displays the spatial patterns of annual average PM levels across China. The 10 contrast sites in the northern region had significantly higher concentrations of $PM_{2.5}$ and PM_{10} than the 13 southern sites (levels averaged 19 and 48 μg m^{-3} higher, respectively). The same pattern existed for cities ($PM_{2.5}$ and PM_{10} averaged 19 and 58 μg m^{-3} higher in northern cities). Along the east-west axis, PM levels were the highest in the middle region, especially at the middle reaches of the Yellow and Yangtze Rivers. The middle and eastern regions showed similar differences for $PM_{2.5}$ and PM_{10} (23 and 30 μg m^{-3}), suggesting relatively low levels of coarse fraction PM ($PM_{2.5-10}$) in these areas.

High PM concentrations in northern China have been attributed to emissions from fossil fuels and biomass combustion (Wang et al., 2014; Chai et al., 2014; Pui et al., 2014; Gao et al., 2015; Qu et al., 2010), and to topography and meteorology that inhibit dispersion. This region's mineral and coal resources have led to extensive mining, metallurgy, machinery manufacturing and other heavy industry with large emissions. In contrast, the southern region, especially along the coast, has primarily light industry, which consumes less fuel and produces lower emissions. Precipitation levels also follow a strong gradient, with annual levels decreasing from the southeast coastal to northwest inland areas where Aeolian processes promote PM emissions on arid lands, particularly on dry and windy days (Liu et al., 2008). Indeed, northwest sites S8–10 have among the lowest $PM_{2.5}/PM_{10}$ ratios (averaging 0.45 ± 0.05), suggesting large contributions of entrained soil that is predominately coarse fraction PM. The highest PM levels occur in middle China, particularly around the middle reaches of the Yellow and Yangtze Rivers. Notably, $PM_{2.5}$ and PM_{10} concentrations at three contrast sites in this region (S4, S5, S7) average 105 and 184 μg m^3, respectively, twice that at most other sites. Levels at S5 and S7 (Zhengzhou and Xi'an) contrast sites also exceeded city-wide levels. This region has a large population, extensive economic activity and sizable emissions from coal-fired power plants, industry and traffic. Remote sensing of $PM_{2.5}$ also shows that this is the most polluted area in China (Peng et al., 2016). While air quality in most Chinese cities has been improving recently (Ministry of Environmental Protection of the People's Republic, 2016), air quality in middle China appears to be further degrading as poorly-controlled coal-fired power plants and industry move to this region.

For $PM_{2.5}$, the variation within a region (both between nearby cities and between cities and their contrast sites) was relatively modest. This reflects the widespread distribution of emission sources, the regional nature of both inorganic and organic secondary aerosols, which comprise a substantial fraction of $PM_{2.5}$ (Zheng et al., 2014), and the relatively long atmospheric lifetime of $PM_{2.5}$ (Hu et al., 2014).

3.2. Daily PM levels

Daily $PM_{2.5}$ and PM_{10} concentrations across the 23 site pairs are summarized in Table 2. The daily Grade II Standards were frequently exceeded, e.g., the $PM_{2.5}$ standard (75 μg m^{-3}) was exceeded on 32% of days in cities and on 23% (range from 1 to 58%) of days at contrast sites, while the PM_{10} standard (150 μg m^{-3}) was exceeded on 23% of days in cities and on 15% (range from 0 to 60%) of days at contrast sites. The most polluted areas included S5 Zhengzhou, S4 Shijiazhuang and S7 Xi'an. Excluding the three sites with high contrast measurements (S5, S7, S22), the median ratio of daily $PM_{2.5}$ concentrations at contrast to city sites was 0.72 ± 0.19 and slightly lower for PM_{10}, 0.68 ± 0.20, similar to ratios of annual averages.

Daily $PM_{2.5}$ and PM_{10} levels were strongly correlated (Spearman correlation coefficients averaged 0.90 and 0.87 at city and contrast sites, respectively). Daily $PM_{2.5}$ levels at urban and contrast sites were also highly correlated (average: 0.87; range: 0.61 to 0.97); daily PM_{10} levels at most urban and contrast site pairs had slightly lower correlation (Table 2). High correlation between PM size fractions can indicate common emission sources and sometimes common meteorological influences on concentrations (Zhang et al., 2016b; Nikolaos et al., 2016; Li et al., 2016; Bisht et al., 2015; Shen et al., 2014; Dimitriou & Kassomenos, 2014). In contrast, lower correlation coefficients at the western (S9 Lanzhou) contrast site may reflect emissions of windborne dust that are largely uncorrelated with $PM_{2.5}$ emissions, which are mostly combustion-related (Zhou et al., 2016). $PM_{2.5}/PM_{10}$ ratios increased when $PM_{2.5}$ levels were high, e.g., during exceedances of the Grade II $PM_{2.5}$ standard, this ratio averaged 0.69 ± 0.09 at the city sites, compared to 0.54 ± 0.09 when the standard was attained. The contrast sites showed comparable trends. In part, these patterns reflect the seasonal variation of PM levels (discussed later).

Daily urban increments differed by site and PM concentration. Fig. 3 shows the average $PM_{2.5}$ urban increment by decile of the city

Table 2
Statistics of daily average concentrations at city and contrast sites. Shows 75th and 90th percentile concentrations; frequency of exceeding Grade II standards, and Spearman correlation coefficients between $PM_{2.5}$ and PM_{10} concentrations by site. Right-hand columns show median ratios of contrast to city concentrations for $PM_{2.5}$ and PM_{10}, and Spearman correlation coefficients between contrast and city sites for $PM_{2.5}$ and PM_{10}. For each variable, values above the 75th percentile are shown in bold; values under the 25% percentile are shown in italics.

	Urban sites								Contrast sites								Contrast - urban sites			
	Concentration (μg/m^3)				Freq > standard			Correl	Concentration (μg/m^3)				Freq > standard			Correl	Med. ratio con/urban		Correlation coefficient	
Site	$PM_{2.5}$		PM_{10}		$PM_{2.5}$	PM_{10}	Either	$PM_{2.5}$	$PM_{2.5}$		PM_{10}		$PM_{2.5}$	PM_{10}	Either	$PM_{2.5}$				
Code	75th	90th	75th	90th	(%)	(%)	(%)	PM_{10}	75th	90th	75th	90th	(%)	(%)	(%)	PM_{10}	$PM_{2.5}$	PM_{10}	$PM_{2.5}$	PM_{10}
S1	100	160	145	208	32	22	33	0.93	84	142	119	181	28	16	29	**0.93**	0.81	0.78	**0.97**	**0.97**
S2	80	127	141	202	27	21	31	*0.84*	67	124	107	169	21	13	28	0.87	0.81	0.56	0.89	0.80
S3	**117**	**164**	143	203	44	23	44	0.92	91	**143**	115	168	32	14	35	0.89	0.73	0.73	**0.96**	0.90
S4	**191**	**301**	**366**	**501**	**72**	**83**	**85**	0.89	**130**	**187**	**250**	**320**	**52**	**60**	**83**	0.88	0.69	0.68	0.88	0.81
S5	**124**	**181**	**194**	**244**	**60**	**48**	**63**	0.90	**127**	**188**	**206**	**279**	**58**	**51**	**65**	0.85	**0.99**	**1.02**	**0.94**	0.88
S6	79	111	170	**218**	28	**33**	37	*0.81*	68	103	126	159	21	12	**41**	*0.77*	0.74	0.62	0.89	*0.75*
S7	110	**172**	**191**	**286**	**47**	**47**	**56**	0.88	**140**	**236**	**227**	**347**	**56**	**57**	**61**	*0.83*	**1.14**	**1.12**	0.88	*0.73*
S8	*64*	*93*	138	190	*18*	20	25	*0.86*	*34*	*54*	*76*	115	*3*	3	20	*0.84*	0.58	0.57	*0.81*	0.80
S9	78	102	**174**	218	28	**37**	45	*0.76*	52	78	132	172	11	15	**41**	*0.64*	0.68	0.80	*0.64*	*0.65*
S10	78	96	159	198	28	31	41	*0.77*	70	91	**134**	167	20	15	36	*0.78*	0.82	0.76	*0.61*	*0.66*
S11	**118**	**173**	**183**	**254**	**54**	**37**	**54**	**0.96**	76	105	97	125	25	4	38	0.91	0.64	0.56	*0.84*	0.83
S12	90	134	126	179	33	17	34	**0.96**	52	82	85	131	12	5	20	**0.95**	0.59	0.62	0.89	**0.92**
S13	*67*	*93*	*96*	*125*	*19*	*4*	*19*	0.94	*45*	*69*	*67*	*89*	*8*	*0*	*8*	**0.93**	0.62	0.62	0.90	0.84
S14	*51*	*66*	*98*	*123*	*6*	*2*	*6*	0.89	*31*	*39*	*52*	*66*	*1*	*0*	*3*	0.92	0.61	0.56	*0.85*	*0.76*
S15	80	125	122	177	27	17	27	**0.97**	75	109	113	160	25	14	24	**0.95**	**0.93**	**0.88**	**0.95**	**0.94**
S16	68	94	*95*	*126*	21	*4*	*20*	**0.97**	63	83	81	*106*	16	*2*	*18*	0.93	0.84	0.80	0.92	0.88
S17	*42*	*62*	*82*	*101*	*5*	*1*	*5*	0.90	*36*	*47*	*54*	*74*	*2*	*0*	*3*	*0.79*	0.77	0.57	0.88	*0.72*
S18	*45*	*61*	*80*	*101*	*3*	*0*	*3*	0.93	*38*	*51*	*54*	*79*	*3*	*0*	*3*	**0.93**	0.81	0.62	*0.75*	0.78
S19	*43*	*66*	*69*	*92*	*8*	*1*	*7*	**0.95**	*32*	*59*	*58*	*92*	*4*	*1*	*4*	**0.93**	**0.88**	0.82	**0.94**	**0.90**
S20	101	161	133	189	**48**	18	46	*0.82*	84	139	**135**	**203**	32	**20**	30	0.84	0.83	**0.93**	0.90	0.88
S21	**112**	**185**	**174**	**231**	**49**	32	**48**	0.93	**94**	**153**	126	**182**	**36**	**17**	38	0.85	0.84	0.81	0.92	**0.90**
S22	97	150	118	151	39	11	29	0.91	**104**	**145**	125	156	**41**	11	31	0.92	**0.94**	**1.01**	0.89	**0.91**
S23	**114**	155	147	199	45	24	**46**	**0.96**	**100**	139	**137**	**188**	**37**	**21**	**40**	0.93	**0.89**	**0.93**	**0.93**	0.88
Ave.	89	132	145	196	32	23	35	0.90	74	112	116	162	24	15	30	0.87	0.79	0.75	0.87	0.83
St. Dev.	34	55	60	84	18	19	20	0.06	32	51	53	73	17	18	21	0.08	0.14	0.17	0.09	0.09

concentration at each site pair. Several important patterns are seen. First, several site-pairs have much higher urban increment fractions (e.g., S8, S12–14; also shown in Table 3). Second, most sites show modest urban increments at most deciles, but sometimes much higher concentrations and/or increments at the top deciles, reflecting skewed concentration distributions (especially sites S1, S3, S4, S7, S9, S11–12, S20–22). Third, the top deciles at cities S4 and S11 have very large urban increments, suggesting that city emissions are responsible for much or most of the pollution on the highest pollution days, which differs from the other cities where high pollution days have high levels at contrast sites. Fourth, during low pollution days in several cities (including S5, S7 and S22 where levels at contrast sites exceeded city levels, as well as S15, S20 and S23), $PM_{2.5}$ is nearly entirely due to background levels. A parallel analysis for PM_{10} (SM Fig. S4) shows similar features: many of the same sites have skewed distributions (especially S1–3, S5, S7, S9, S20, S23); most sites have an approximately constant fraction for the urban increment, although the urban increment tends to increase in the top decile; and several sites are dominated by background, especially at lower concentrations (S5, S7, S9, S20, S22).

Elevated concentrations of $PM_{2.5}$ and PM_{10} often occurred across large regions. For example, during a serious "haze" episode lasting 15 days (February 12 to 26, 2014) over 15 provinces (18.1 million km^2) (Sohu Company, 2014), daily $PM_{2.5}$ concentrations exceeded 75 μg m^{-3} for 10 or more days in 10 of the 23 cities studied; In one of the most polluted cities (S4 Shijiazhuang), daily $PM_{2.5}$ and PM_{10} concentrations exceeded 500 and 700 μg m^{-3}, respectively. Typically, urban and contrast sites showed similar trends (SM Fig. S5). In one of the less polluted cities, S19 Haikou, the southern-most city located over 1000 km distant, $PM_{2.5}$ and PM_{10} levels were much lower during this period, but daily trends still reflected the temporal pattern (with a 1-day lag) seen at Shijiazhuang.

Daily $PM_{2.5}$ and PM_{10} concentrations in different cities were moderately to highly correlated (Spearman correlation coefficients R_{SP} averaged 0.33 and 0.39, respectively). Typically, correlation was higher between closer cities, e.g., those in the same region, while correlations between distant sites in the southern and northern regions were negligible (SI Table S4), matching the spatial autocorrelation results. Correlations across the contrast sites were lower (e.g., correlations for $PM_{2.5}$ and PM_{10} averaged 0.31 and 0.27, respectively); again, correlations were higher between closer cities. The higher correlations for $PM_{2.5}$ reflect its boarder distribution noted earlier, and the higher correlation among city sites suggests correlated anthropogenic emissions and/or dispersion influences. Lower correlations with other sites were seen at S14 Kunming in the southwest, due to its special environment (e.g., ringed by the northern plateau and mountains on three sites) and S3 Beijing, which was correlated with several northern cities (S4, S6), but generally uncorrelated with the southern cities.

The factor analysis identified sites that had similar temporal trends and potentially similar influences on PM concentrations. Fig. 4 depicts factor loadings for $PM_{2.5}$ and PM_{10} at the contrast sites using pie charts, and shows how PM levels at the sites contribute to each factor. (Additional factor analysis results are in SM Table S5). For example, $PM_{2.5}$ factor 1 (red slices in Fig. 4, left) represents large loadings at sites S13–19 and S22, meaning that $PM_{2.5}$ fluctuations at these southern sites were highly correlated and potentially influenced by common processes. Five factors explained 75% of the variance in the $PM_{2.5}$ concentrations at the contrast sites: factor 1 (noted earlier) included southern and several nearby inland sites and explained 43% of the variance; factor 2 included northern sites S2–8 but not S4 (which had the highest concentrations and a large urban increment as discussed above) and explained 16% of the variance; factor 3 included central sites S20–23 (S20 and S22 had loadings just slightly below 0.5) and explained 7%; factor 4 included western and middle sites S10–12 and S20–21 and accounted for 5% of the variance; and factor 5 included only two cities and explained 5% of the variance. For PM_{10}, five factors also explained 75% of the variance: factor 1 included southern sites (except S16) and some nearby inland sites (S14–15, S17–19, S22–23; 41% of variance); factor 2 included some of northern sites (S3-S6, S8; 14%); and factor 3 included western sites (S10, S12–13, S15–16; 9%). These three PM_{10} factors were nearly identical to the first three $PM_{2.5}$ factors. Factors 4 and 5 for PM_{10} explained 7 and 5%

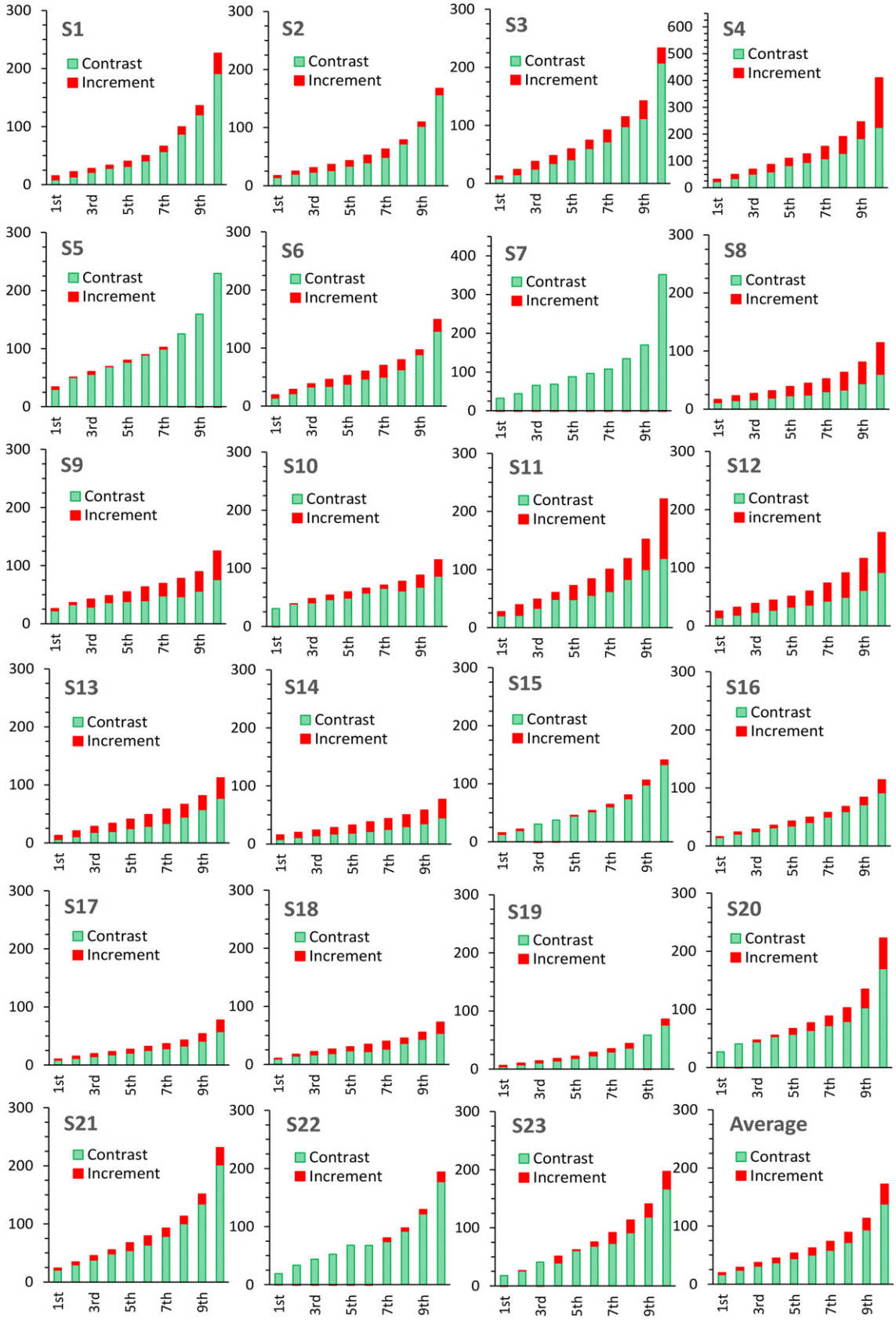

Fig. 3. Average contrast site concentration (green) and urban increment (red) of $PM_{2.5}$ concentrations in μg m^{-3} by decile at each site pair, plus 23-site average (bottom right). Based on daily data. S4 and S7 use different scales.

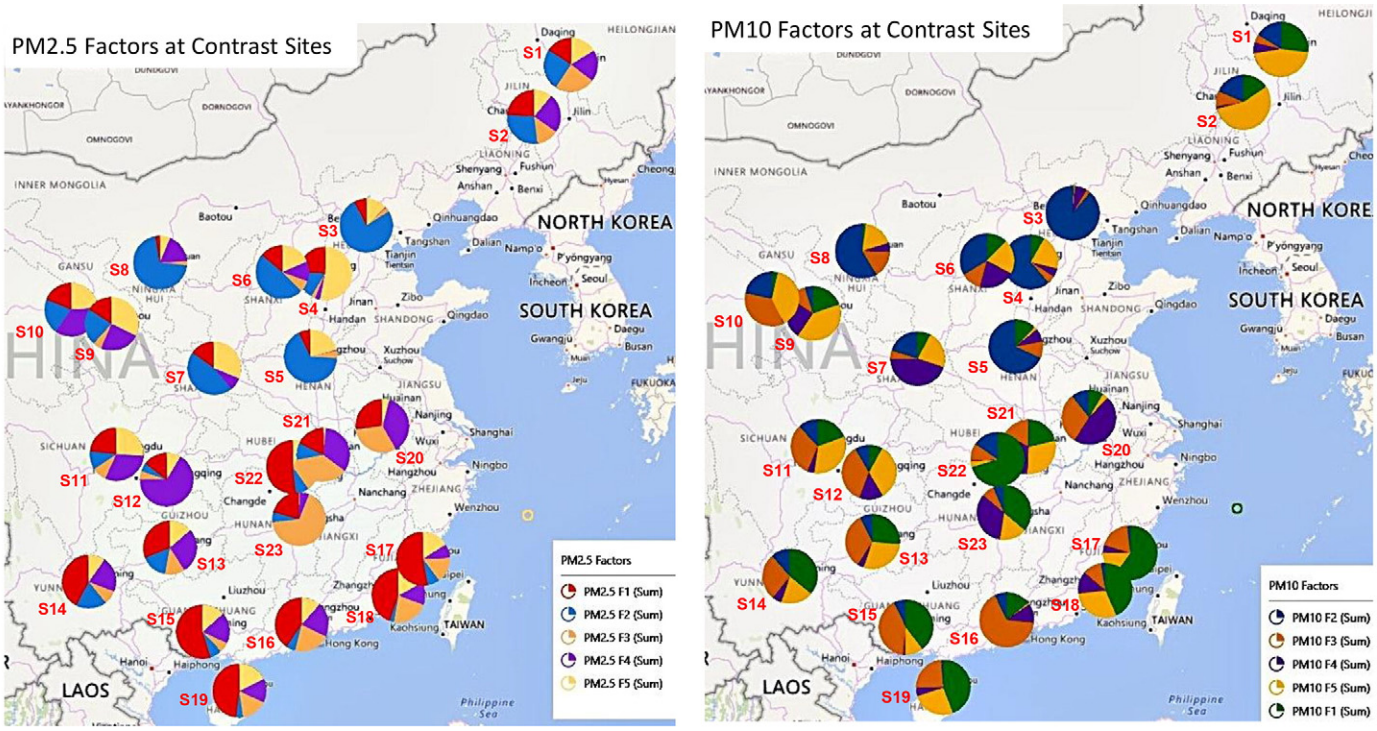

Fig. 4. Factor analysis results for contrast sites for $PM_{2.5}$ (left) and PM_{10} (right). Pie diagram at each site apportions normalized and absolute factor loadings determined using daily PM data.

of the variance, respectively. These results showed some sensitivity regarding data treatment (e.g., whether data was imputed, averaging time, ranked or unranked concentrations, and city or contrast sites), particularly for the minor factors 4 and 5 (SM Table 5), however, results for the three largest factors remained very similar.

The factor analysis groupings often, but not always, followed geographic regions. The analysis provides a check on the appropriateness of the geographic groups, simplifies and interprets the correlation coefficient matrix (SM Table S4), and provides alternative groupings. Results from these and other clustering and data reduction techniques are interpretative, i.e., not necessarily unique or subject to hypothesis testing.

3.3. Seasonal and day-of-week variation

All sites showed considerable seasonal variation in $PM_{2.5}$ and PM_{10} levels. Monthly trends for the sites in groups 1–3 (southern, northern, and middle regions, respectively) identified by the factor analysis just discussed are shown in Fig. 5. (Seasonal averages at all sites are shown in Table S2). $PM_{2.5}$ and PM_{10} concentrations were highest in winter and lowest in summer, patterns that applied at both city and contrast sites and in each region. Differences between winter and summer months were dramatic, e.g., 2-fold differences in PM_{10} concentrations and 3-fold differences in $PM_{2.5}$ occurred across large regions. Yet larger changes were observed for urban $PM_{2.5}$ increments, which increased 5-fold (to 43 and 53 μg m^{-3}) at the northern and middle cities. In December and January, stagnant meteorological conditions including inversions are common, which retard the dilution and transport of pollutants, and poorly controlled coal combustion for domestic heating is at its peak. In contrast, in July and August, the boundary layer is high and precipitation is common, factors that can lower concentrations. PM levels were also elevated in October, likely due to agricultural biomass burning. In April and May, particularly at the northwest sites, another concentration peak appears, likely due to sand and dust storms in Mongolia and northwest China (Zhou et al., 2016).

Some of the differences in the monthly trends among the three site groupings in Fig. 5 can be attributed to climatic differences, e.g., the southern region of China ends its cold season earlier than the north, which may explain the lower PM levels seen for group 1 in February and March. Multiyear analyses would help to confirm seasonal trends. Despite the much lower concentrations in summer, Grade II $PM_{2.5}$ standards were exceeded on an average of 9 days in each of the 23 cities (range: 0–49 days) in the summer months (June – August), while Grade II PM_{10} standards were exceeded an average of 7.5 times (range: 0–66 days).

The $PM_{2.5}/PM_{10}$ ratios show some seasonality. These ratios decrease slightly in summer (Fig. 5), indicating a higher fraction of coarse PM, probably due to entrainment of dust during dry and windy conditions, especially in the northern and western regions. In winter, the elevated ratio combined with the high PM concentrations (especially the urban $PM_{2.5}$ increment) suggests the importance of secondary $PM_{2.5}$ (Hu et al., 2014).

The ratio of PM levels at contrast to urban sites did not show seasonal variation. As shown for annual averages, the average seasonal ratios for $PM_{2.5}$ (0.78–0.80) were very similar to those for PM_{10} (0.77–0.79). However, the variation among sites for the PM_{10} ratio increased in summer and fall, largely due to increases in concentrations at contrast sites S5 and S7, two of the three sites noted earlier where annual concentrations exceeded levels at the corresponding urban sites. The summer and fall increase in coarse fraction PM levels at these sites may be due to local sources of entrained soil or dust.

A number of day-of-week and weekend-weekday effects were observed. In many cities, Wednesdays and Thursdays had the lowest concentrations, and Saturdays and Sundays the highest. Weekend concentrations exceeded weekday levels at most cities, but differences were statistically significant at only five cities (S2–3, S5–6, S20) where $PM_{2.5}$ and PM_{10} concentrations averaged 18 and 11% higher, respectively, on weekends (1-sided Mann-Whitney tests; SM Table S6, SM Fig. S6). For $PM_{2.5}$, weekend-weekday differences increased to 21% in winter at the five sites showing significant differences (S1, S10, S17–18, S28); interestingly, levels at contrast sites of these cities (as well as at S2) were 27% higher on weekends (SM Fig. S6). Other seasons showed smaller and fewer differences. These results suggest additional emissions on weekends that affect $PM_{2.5}$ levels, probably associated with additional traffic on weekends, though heating and cooking might contribute. Day-of-week and in particular weekday/weekend differences have been

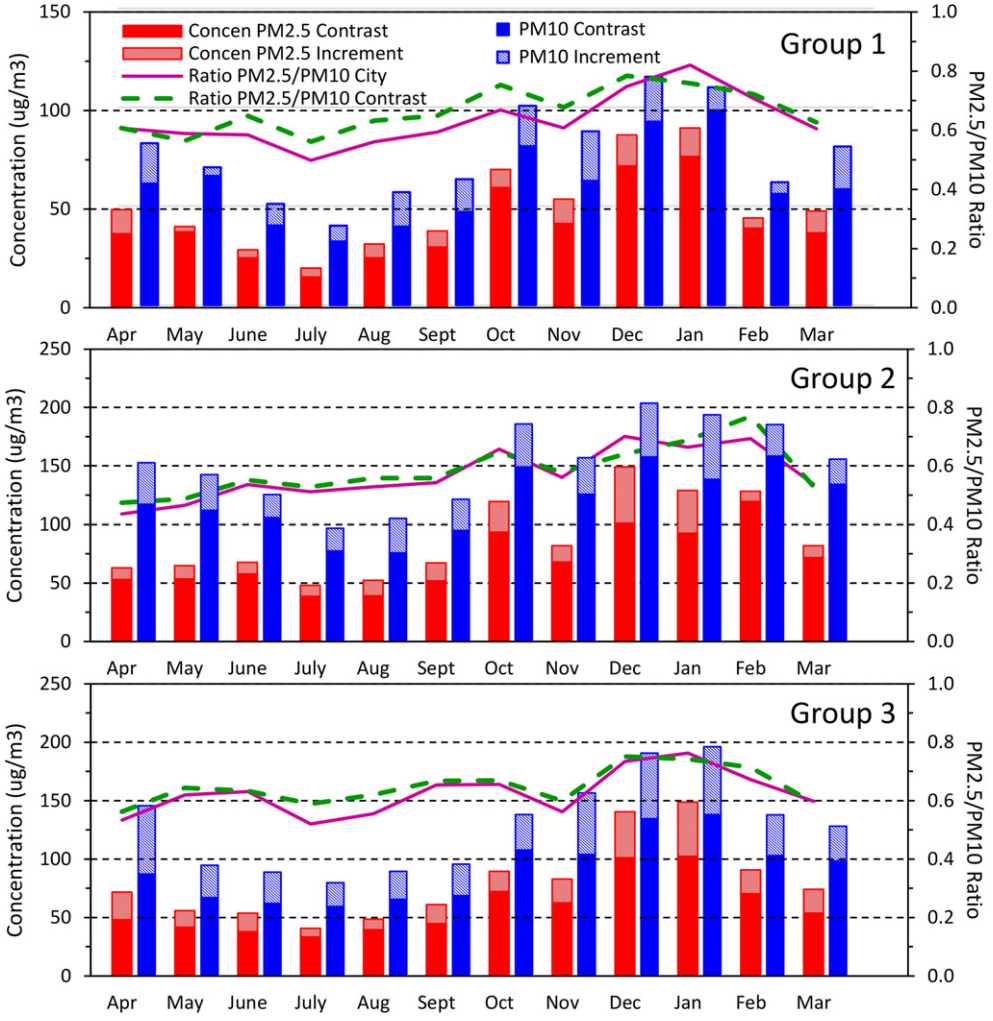

Fig. 5. Average concentrations and $PM_{2.5}/PM_{10}$ ratios by month at group 1 (southern; S13-S19, S22–23), group 2 (northern sites; S1–8), and group 3 (middle, S10–12, S21–22) sites. Scale for group 1 is smaller than for groups 2 and 3. Groups based on factor analysis results.

observed and related to traffic-related and other emissions (Zha et al., 2014; Zhao et al., 2013; Sabaliauskas et al., 2013; Dutton et al., 2010); other sites do not show differences (Hu et al., 2014; Shen et al., 2014). Our findings suggest that emission rates in some Chinese cities undergo day-of-week variation, and the weekly pattern (e.g., high levels on weekends, low levels on Wednesdays and Thursdays) is somewhat unusual and not fully explained.

4. Discussion

The analysis of recent PM data at the 23 city-contrast pairs shows air quality concerns in China at city, regional and national levels. While cities in southern China had lower PM levels, daily and annual standards were exceeded throughout the country. All sites showed large seasonal differences in PM concentrations, and most showed very high correlation between $PM_{2.5}$ and PM_{10}, and high ratios of $PM_{2.5}/PM_{10}$. In northern and middle China, elevated PM concentrations, generally modest urban increments, and the high correlation between concentrations at urban and contrast sites suggest widespread deterioration of air quality in upwind areas. While emission inventories were not investigated in this work, possible or probable emission sources include industry and agriculture in exurban areas, as well as upwind cities. In most cities and on most days, high concentrations of $PM_{2.5}$ at the contrast sites, the high $PM_{2.5}/PM_{10}$ ratios, the modest urban increments, and the correlations between concentrations at contrast sites suggest that regional or exurban sources of $PM_{2.5}$ dominate both $PM_{2.5}$ and PM_{10} levels throughout the year. However, conditions in a few cities differ, e.g., S4 Shijiazhuang, S11 Chengdu and S12 Chongqing have large urban increments during high pollution days, suggesting strong and localized emission sources.

Monitoring at the contrast sites was intended to portray air quality upwind of the city. However, annual average PM concentrations at three contrast sites exceeded levels at the corresponding downwind cities, indicating that these sites do not serve their intended purpose and that different locations for the contrast sites are needed. More generally, a single contrast site may not accurately portray background levels for several reasons. First, a single site cannot be upwind all of the time. Second, recirculating winds, particularly with low wind speed conditions, may diminish concentration differences between city and contrast sites. Third, nearby and other upwind sources may affect the contrast site. These sources may be relatively small, e.g., related to construction, or much larger but more distant. Fourth, secondary formation of $PM_{2.5}$ occurs over large scales, and even if the site is upwind, $PM_{2.5}$ levels may continue to evolve as air travels past the contrast site to the city, potentially increasing the urban increment. Despite these issues, urban increments were observed at most sites, although their magnitude was generally modest, averaging only 17% of the city concentration. This suggests the strength and importance of regional $PM_{2.5}$ and PM_{10} sources and regional or long range transport. These inferences could be confirmed by the collection and analysis of PM at more distant "regional background" sites, stratifying levels by meteorological conditions, and using dispersion modeling and receptor models for source apportionments. In addition, daily PM data were highly autocorrelated.

We previously showed that in Beijing the best predictor of the next day's concentration is the current day's concentration (Batterman et al., 2016). This also applies to PM levels at other city and contrast sites, and it affects day-to-day variability.

Controls on PM emissions are required to reduce concentrations and achieve air quality standards. The analysis suggests that both urban and regional sources need controls, particularly for $PM_{2.5}$. In September 2013, China issued the "Action Plan on Prevention and Control of Air Pollution", which called for reductions in PM_{10} concentrations in larger cities (above prefecture level) of at least 10% from 2012 levels by 2017; $PM_{2.5}$ levels in Beijing-Tianjin-Hebei Province, the Yangtze River Delta and the Pearl River Delta are to be reduced by 25, 20 and 15%, respectively; and annual $PM_{2.5}$ concentration in Beijing are to attain 60 $\mu g\ m^{-3}$ (The Central People' s Government of the People's Republic of China, 2013). Our results, including the ratios of contrast/city concentrations, suggest that a 10% reduction in PM_{10} levels can be achieved by local emission reductions in most cities (possibly difficult at Zhengzhou, Changsha, Zhuzhou, Hefei and Yinchuan), however, reductions of 20% or higher may be difficult (especially in Beijing) unless background levels also are lowered. Attainment of air quality standards in cities is feasible if both urban and exurban/regional sources control both primary PM and PM precursors (e.g., SO_2).

5. Conclusions

PM pollution is recognized as a serious problem in Chinese cities. While not as well recognized, measurements at contrast sites located outside of cities also show that PM pollution is a serious concern in the surrounding countryside. This study examines the spatial and temporal variation of PM levels and quantifies the background (or regional) component using an unusually complete record of daily $PM_{2.5}$ and PM_{10} concentrations in 23 cities and the corresponding contrast sites. Annual $PM_{2.5}$ and PM_{10} concentrations at the 23 contrast sites averaged 57 ± 26 $\mu g\ m^{-3}$ and 91 ± 44 $\mu g\ m^{-3}$, respectively; levels in the 23 cities were higher by only 13 and 25 $\mu g\ m^{-3}$, respectively. No contrast site attained Chinese Grade I (or IT-3) standard or the WHO Air Quality Guideline, and only five sites met the Grade II (IT-1) standard. With exceptions of Haikou, Fuzhou and Xiamen (PM_{10}), all cities and contrast sites exceeded the annual average Grade II standards for both $PM_{2.5}$ and PM_{10}. The daily Grade II standards for $PM_{2.5}$ and PM_{10} were frequently exceeded. Most cities had small urban increments, high correlation between $PM_{2.5}$ and PM_{10} concentrations, and high correlation between concentrations at city and contrast sites. In a few cities, PM levels were significantly affected by urban sources, but only on days with the highest concentrations. PM levels were correlated across broad areas, but levels and trends varied by region, and the highest levels were found in northern and middle China. All sites demonstrated dramatic seasonal changes (much higher in winter months), and several sites (mostly in cities) showed day-of-week effects. Overall, these results highlight the dominance of regional sources of $PM_{2.5}$ at city and contrast sites. These sources will require emission controls to achieve air quality goals, in particular, the PM_{10} and $PM_{2.5}$ targets announced by the Chinese government in 2013. In addition, continued monitoring and analysis of PM are needed to support air quality goals and pollution control strategies.

Acknowledgments

This study was supported by Fujian Social Sciences Planning Project (Grant No. FJ2016C036), Fujian Education and Scientific Research Project for Young and Middle-aged Teachers (Grant No. JAT160567), Social Science Research Plan, Fujian Province Department of Science and Technology (Grant No. 2015R0099), Plan of Environmental Protection Science and Technology, Fujian Province, P.R. China (Grant No. 2013R003), S. Batterman acknowledges support from the National Institutes of Health (National Institute of Environmental Health Sciences (NIEHS)) P30ES017885 and National Institute for Occupational Safety and Health (NIOSH) 5T42OH008455. The authors declare they have no actual or potential competing financial interests.

Appendix A. Supplementary data

Supplementary data to this article can be found online at http://dx.doi.org/10.1016/j.scitotenv.2017.05.048.

References

Batterman, S., et al., 2016. Characteristics of $PM_{2.5}$ concentrations across Beijing during 2013–2015. Atmos. Environ. 145, 104–114.
BestApp Studio, 2016. PM25 Homepage. BestApp Studio, Guangzhou, China Accessed at. http://pm25.in/.
Bisht, D.S., et al., 2015. Aerosol characteristics at a rural station in southern peninsular India during CAIPEEX-IGOC: physical and chemical properties. Environ. Sci. Pollut. Res. 22 (7), 5293.
Chai, F., et al., 2014. Spatial and temporal variation of particulate matter and gaseous pollutants in 26 cities in China. J. Environ. Sci. (China) 26 (1), 75–82.
Chen, Y., et al., 2013. Evidence on the impact of sustained exposure to air pollution on life expectancy from China's Huai River policy. Proc. Natl. Acad. Sci. U. S. A. 110 (32), 12936–12941.
Dimitriou, K., Kassomenos, P., 2014. Decomposing the profile of PM in two low polluted German cities - mapping of air mass residence time, focusing on potential long range transport impacts. Environ. Pollut. 190, 91–100.
Dutton, S.J., et al., 2010. Temporal patterns in daily measurements of inorganic and organic speciated $PM_{2.5}$ in Denver. Atmos. Environ. 44 (7), 987–998.
Fu, Q., et al., 2010. Source, long-range transport, and characteristics of a heavy dust pollution event in Shanghai. J. Geophys. Res. Atmos. 115 (21) p. np.
Gao, J., et al., 2015. The variation of chemical characteristics of PM2.5 and PM10 and formation causes during two haze pollution events in urban Beijing, China. Atmos. Environ. 107, 1.
Hu, J., et al., 2014. Spatial and temporal variability of $PM_{2.5}$ and PM10 over the North China Plain and the Yangtze River Delta, China. Atmos. Environ. 95, 598–609.
Jahn, H.J., et al., 2013. Ambient and personal PM2.5 exposure assessment in the Chinese megacity of Guangzhou. Atmos. Environ. 74, 402–411.
Jakubiak-Lasocka, J., et al., 2015. Impact of traffic-related air pollution on health. Adv. Exp. Med. Biol. 834, 21–29.
Lai, P.C., So, F.M., Chan, K.W., 2009. Spatial Epidemiological Approaches in Disease Mapping and Analysis. xx. CRC Press, Boca Raton 174 p., [10] p. of plates.
Lai, S.C., et al., 2016. Characterization of PM2.5 and the major chemical components during a 1-year campaign in rural Guangzhou, Southern China. Atmos. Environ. 167, 208.
Li, H., et al., 2016. Size-dependent characterization of atmospheric particles during winter in Beijing. Atmosphere 7 (3), 36.
Liu, H., et al., 2008. A research of Aeolian landform in northern China based on remote sensing imagery. Geogr. Res. 27 (1), 109–118.
Ma, Z.W., et al., 2016. Satellite-Based Spatiotemporal Trends in PM2.5 Concentrations: China, 2004–2013. Environ. Health Perspect. 124 (2), 184.
Ministry of Environmental Protection of the People's Republic, 2016l. China Environmental Statement. Ministry of Environmental Protection of the People's Republic, Beijing, China Accessed at. http://www.mep.gov.cn/hjzl/.
Ministry of Environmental Protection of the People's Republic of China, 2012l. Setting Schemes of National Environmental Air Monitoring Network(above prefecture level). Ministry of Environmental Protection of the People's Republic of China, Beijing, China Accessed at. http://www.zhb.gov.cn/gkml/hbb/bwj/201204/t20120401_250935.htm.
Ministry of Environmental Protection of the People's Republic of China, 2013l. Technical Specifications for Installation and Acceptance of Ambient Air Quality Continuous Automated Monitoring System for PM10 and PM2.5 (HJ 655-2013). Ministry of Environmental Protection of the People's Republic of China, Beijing, China Accessed at. http://kjs.mep.gov.cn/hjbhbz/bzwb/dqhjbh/jcgfffbz/201308/t20130802_256855.htm.
National Bureau of Statistics of China, 2016. National Data. National Bureau of Statistics of China, Beijing, China Accessed at. http://data.stats.gov.cn/easyquery.htm?cn=E0103.
Nikolaos, B., et al., 2016. Particulate matter levels and comfort conditions in the trains and platforms of the Athens underground metro. AIMS Environmental Science 3 (2), 199.
Peng, J., et al., 2016. Spatiotemporal patterns of remotely sensed PM2.5 concentration in China from 1999 to 2011. Remote Sens. Environ. 174, 109.
$PM_{2.5}$ Real-time Monitoring Net, Fujian, China, 2013. Accessed at. http://www.pm25china.net/.
Pui, D.Y.H., Chen, S.-C., Zuo, Z., 2014. PM2.5 in China: Measurements, sources, visibility and health effects, and mitigation. Particuology 13, 1–26.
Qu, W.J., et al., 2010. Spatial distribution and interannual variation of surface PM10 concentrations over eighty-six Chinese cities. Atmos. Chem. Phys. 10, 5641–5662.
Sabaliauskas, K., et al., 2013. Cluster analysis of roadside ultrafine particle size distributions. Atmos. Environ. 70, 64–74.
Seltenrich, N., 2016. A clearer picture of China's Air using satellite data and ground monitoring to estimate PM2.5 over time. Environ. Health Perspect. 124 (2), A38.
Shen, G.F., et al., 2014. Ambient levels and temporal variations of $PM_{2.5}$ and PM_{10} at a residential site in the mega-city, Nanjing, in the western Yangtze River Delta, China. J. Environ. Sci. Health A Tox. Hazard. Subst. Environ. Eng. 49 (2), 171–178.
Shen, Z.X., et al., 2016. Retrieving historical ambient PM2.5 concentrations using existing visibility measurements in Xi'an, Northwest China. Atmos. Environ. 126, 15.
Sohu Company. Sohu Company 2014 (cited 6 January 2016); Available from: http://business.sohu.com/20140308/n396269440.shtml.
Sun, Z., et al., 2013. Assessment of population exposure to PM10 for respiratory disease in Lanzhou (China) and its health-related economic costs based on GIS. BMC Public Health 13.
Tan, J.H., et al., 2009. Chemical characteristics of PM2:5 during a typical haze episode in Guangzhou. J. Environ. Sci. 21, 774–781.
Tan, J.-H., et al., 2014. Source apportionment of size segregated fine/ultrafine particle by PMF in Beijing. Atmos. Res. 139, 90–100.

The Central People' s Government of the People's Republic of China, 2013o. Action Plan on Prevention and Control of Air Pollution. The Central People's Government of the People's Republic of China, Beijing, China Accessed at. http://www.gov.cn/zwgk/2013-09/12/content_2486773.htm.
Wallner, P., Hutter, H.-P., Moshammer, H., 2014. Worldwide associations between air quality and health end-points: are they meaningful? Int. J. Occup. Med. Environ. Health 27 (5), 716–721.
Wang, J., 2014. China Air Quality Online Monitoring and Analysis Platform. $PM_{2.5}$ Scientific Experimental Expert Group, China (cited 6 January 2016). Available from:. http://www.aqistudy.cn/.
Wang, J., et al., 2013. Contamination characteristics and possible sources of PM_{10} and $PM_{2.5}$ in different functional areas of Shanghai, China. Atmos. Environ. 68, 221–229.
Wang, Y., et al., 2014. Spatial and temporal variations of six criteria air pollutants in 31 provincial capital cities in China during 2013–2014. Environ. Int. 73, 413–422.
Wang, L., et al., 2015. Long-range transport and regional sources of PM2.5 in Beijing based on long-term observations from 2005 to 2010. Atmos. Res. 157, 37.
Wang, F.W., et al., 2016a. Seasonal variation of carbonaceous pollutants in PM2.5 at an urban 'supersite' in Shanghai, China. Chemosphere 146, 238.
Wang, J.Z., et al., 2016b. Characterization of PM2.5 in Guangzhou, China: uses of organic markers for supporting source apportionment. Sci. Total Environ. 550, 961.
Wen, W., et al., 2016. Impact of emission control on PM2.5 and the chemical composition change in Beijing-Tianjin-Hebei during the APEC summit 2014. Environ. Sci. Pollut. Res. 23 (5), 4509.
WHO, 2005. WHO Air Quality Guidelines for Particulate Matter, Ozone, Nitrogen Dioxide and Sulfur Dioxide - Global Update 2005 - Summary of Risk Assessment. World Health Organization, Geneva, Switzerland Accessed at. http://www.who.int/phe/health_topics/outdoorair/outdoorair_aqg/en/.
WHO, 2016. 7 Million Premature Deaths Annually Linked to air Pollution. World Health Organization, Geneva, Switzerland Access at. http://www.who.int/mediacentre/news/releases/2014/air-pollution/.
Xia, T., et al., 2015. Traffic-related air pollution and health co-benefits of alternative transport in Adelaide, South Australia. Environ. Int. 74, 281–290.
Xu, H.M., et al., 2016. Inter-annual variability of wintertime PM2.5 chemical composition in Xi'an, China: evidences of changing source emissions. Sci. Total Environ. 545, 546.
Yang, W.-S., et al., 2016a. An evidence-based assessment for the association between long-term exposure to outdoor air pollution and the risk of lung cancer. Eur. J. Cancer Prev. 25 (3), 163.
Yang, A., et al., 2016b. Children's respiratory health and oxidative potential of PM2.5: the PIAMA birth cohort study. J. Occup. Environ. Med. 73 (3), 154.
Yang, H.N., et al., 2016c. Composition and sources of PM2.5 around the heating periods of 2013 and 2014 in Beijing: Implications for efficient mitigation measures. Atmos. Environ. 124, 378.
Yang, F., et al., 2016d. Anthropogenic and biogenic organic compounds in summertime fine aerosols (PM2.5) in Beijing, China. Atmos. Environ. 124, 166.
Yang, B., et al., 2016e. A geographically and temporally weighted regression model for ground-level PM2.5 estimation from satellite-derived 500 m resolution AOD. Remote Sens. 8 (3), 262.
Yao, L., et al., 2016. Sources apportionment of PM2.5 in a background site in the North China Plain. Sci. Total Environ. 541, 590.
Yong-Ze, S., et al., 2015. Estimating PM2.5 concentrations in Xi'an City using a generalized additive model with multi-source monitoring data. PLoS One 10 (11).
Yorifuji, T., Kashima, S., Doi, H., 2016. Acute exposure to fine and coarse particulate matter and infant mortality in Tokyo, Japan (2002−2013). Sci. Total Environ. 551-552, 66.
Zha, S., et al., 2014. Characteristics and relevant remote sources of black carbon aerosol in Shanghai. Atmos. Res. 135, 159–171.
Zhang, Z.Y., Wong, M.S., Lee, K.H., 2015. Estimation of potential source regions of PM2.5 in Beijing using backward trajectories. Atmos. Pollut. Res. 6 (1), 173.
Zhang, Y., et al., 2016a. Concentrations and chemical compositions of fine particles (PM2.5) during haze and non-haze days in Beijing. Atmos. Res. 174-175, 62.
Zhang, F., et al., 2016b. Spatiotemporal patterns of particulate matter (PM) and associations between PM and mortality in Shenzhen, China. BMC Public Health 16 (1), 215.
Zhao, X.J., et al., 2009. Seasonal and diurnal variations of ambient $PM_{2.5}$ concentration in urban and rural environments in Beijing. Atmos. Environ. 43 (18), 2893–2900.
Zhao, H., et al., 2013. Characteristics of visibility and particulate matter (PM) in an urban area of Northeast China. Atmos. Pollut. Res. 4 (4), 427–434.
Zheng, M., et al., 2005. Seasonal trends in $PM_{2.5}$ source contributions in Beijing, China. Atmos. Environ. 39, 3967–3976.
Zheng, M., et al., 2014. Sources of primary and secondary organic aerosol and their diurnal variations. J. Hazard. Mater. 264, 536–544.
Zheng, S., et al., 2015. Long-term (2001−2012) concentrations of fine particulate matter (PM2.5) and the impact on human health in Beijing, China. Atmos. Chem. Phys. 15 (10), 5715.
Zheng, Y.X., et al., 2016. Estimating ground-level PM2.5 concentrations over three megalopolises in China using satellite-derived aerosol optical depth measurements. Atmos. Environ. 124, 232.
Zhou, B., et al., 2013. Investiga\ting the geographical heterogeneity in PM10-mortality associations in the China Air Pollution and Health Effects Study (CAPES): a potential role of indoor exposure to PM10 of outdoor origin. Atmos. Environ. 75, 217–223.
Zhou, X.H., et al., 2016. Concentrations, correlations and chemical species of PM2.5/PM10 based on published data in China: potential implications for the revised particulate standard. Chemosphere 144, 518.
Zíková, N., et al., 2016. On the source contribution to Beijing PM2.5 concentrations. Atmos. Environ. 134, 84.